

Nonlinear screening and percolative transition in a two-dimensional electron liquid

Michael M. Fogler

Department of Physics, University of California San Diego, La Jolla, California 92093

(Dated: October 5, 2018)

A variational method is proposed for calculating the percolation threshold, the real-space structure, and the ground-state energy of a disordered two-dimensional electron liquid. Its high accuracy is verified against exact asymptotics and prior numerical results. The inverse thermodynamical density of states is shown to have a strongly asymmetric minimum at a density that is approximately the triple of the percolation threshold. This implies that the experimentally observed metal-insulator transition takes place well before the percolation point is reached.

The discovery that a two-dimensional (2D) electron liquid can be a metal at moderate electron density n_e and an insulator at small n_e was a major surprise that questioned our fundamental understanding of the role of disorder in such systems. Today, almost a decade later, it remains a subject of an intense debate.¹ One important reason why the conventional theory fails could be its flawed basic premise of the “good” metal, i.e., a uniform electron liquid slightly perturbed by impurities and defects. Indeed, modern nanoscale imaging techniques^{2,3,4,5} unambiguously showed that low-density 2D electron systems are strongly inhomogeneous, “bad” metals, where effects of disorder are nonperturbatively strong. In particular, depletion regions (DR), i.e., regions where $n(\mathbf{r})$ is effectively zero, exist. They appear when n_e is too small to adequately compensate fluctuating charge density of randomly positioned impurities. As n_e is reduced in the experiment, e.g., in order to approach the vicinity of the metal-insulator transition (MIT), the DRs are expected to grow in size and concentration and eventually merge below some percolation threshold $n_e = n_p$. An important and controversial issue is whether or not this percolation transition plays any role in the observed MIT.¹ To resolve it one needs to have a theory that is able to calculate n_p and that can describe the inhomogeneous structure of the 2D metal at $n_e \sim n_p$. A great progress in this direction has been achieved by Efros, Pikus, and Burnett,⁶ whose paper is intellectually tied to earlier work on nonlinear screening by Efros and Shklovskii.⁷ Still, analytical results remained scanty and numerical simulations^{6,8} were the only known way to quantitatively study the $n_e \sim n_p$ regime. These simulations are very time consuming and redoing them in order to get any information beyond what is published^{6,8} or to study novel experimental setups seems impracticable. Below I will show that a variational approach to the problem can be a viable alternative. Comparing it with the available numerical results for a typical model of the experimental geometry (Fig. 1), I establish that it correctly predicts the value of n_p and accurately reproduces the energetics of the ground state, in particular, the density dependence of the electrochemical potential μ and of the inverse thermodynamical density of states (ITDOS), $\chi^{-1} = d\mu/dn_e$, over a broad range of n_e . The most striking feature of the resultant function $\chi^{-1}(n_e)$ is a strongly asymmetric minimum, which is observed in real experiments.^{9,10,11,12}

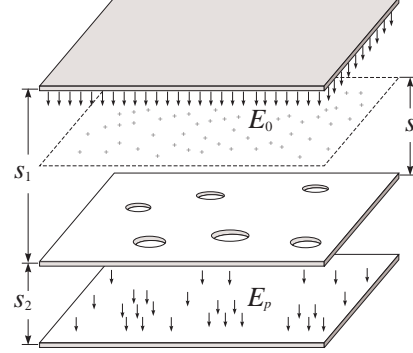


FIG. 1: The geometry of the theoretical model. The 2D layer of interest is sandwiched between the top and the bottom metallic gates. The dopants reside in the plane with the dashed border. The depletion regions (shown as holes in the probed layer) enhance the penetrating electric field E_p .

I will elaborate on the origin of this feature and show that it occurs at $n_e \approx 3n_p$ largely independently of the parameters of the system. Recently, this minimum attracted much interest when Dultz *et al.*¹⁰ reported that in some samples it virtually coincides with the apparent MIT. The proposed theory indicates that, at least for these samples, any connection between the MIT and the percolation of the DRs can be ruled out. Thus, the explanation of the MIT lies elsewhere.

The Hamiltonian of the model is adopted from Efros, Pikus, and Burnett (EPB)⁶ (see also Fig. 1),

$$H = \int d^2r \left\{ \frac{1}{2} [n(\mathbf{r}) - n_e] \Phi(\mathbf{r}) + H_0(n) \right\} \quad (1)$$

where $\Phi(\mathbf{r})$ is the electrostatic potential,

$$\Phi = \int d^2r' \frac{e^2}{\kappa} \left[\frac{n(\mathbf{r}') - n_e}{|\mathbf{r}' - \mathbf{r}|} - \frac{n_d(\mathbf{r}') - n_i}{\sqrt{(\mathbf{r}' - \mathbf{r})^2 + s^2}} \right] \quad (2)$$

κ is the dielectric constant, and $H_0(n)$ is the energy density of the uniform liquid of density n ,

$$H_0(n) = -(e^2/\kappa)n^{3/2}h_0(n). \quad (3)$$

At low densities, $h_0(n) \sim 1$ is a slow function¹³ of n . The negative sign in Eq. (3) reflects the preva-

lence of the exchange-correlation energy over the kinetic one in this regime. The potential created by the random concentration of dopants $n_d(\mathbf{r})$ can be expressed in terms of the effective *in-plane* background charge $\tilde{\sigma}(\mathbf{q}) = \tilde{n}_d(\mathbf{q}) \exp(-qs)$ (the tildes denote the Fourier transforms). With these definition, $\Phi(\mathbf{r})$ coincides with the potential created by the charge density $\sigma(\mathbf{r}) = n(\mathbf{r}) - n_e - \sigma(\mathbf{r})$. I will assume that the dopants have the average concentration $\langle n_d \rangle \equiv n_i \gg s^{-2}$ and are uncorrelated in space. In this case the one- and two-point distribution functions of $\sigma(\mathbf{r})$ have the Gaussian form,

$$P_1(\sigma) = (2\pi K_0)^{-1/2} \exp(-\sigma^2/2K_0), \quad (4)$$

$$P_2 = \frac{1}{2\pi\sqrt{K_0^2 - K_r^2}} \exp\left[\frac{2K_r\sigma\sigma' - K_0(\sigma^2 + \sigma'^2)}{2(K_0^2 - K_r^2)}\right] \quad (5)$$

where $\sigma' = \sigma(\mathbf{r} + \mathbf{r}')$ and K_r is given by

$$K_r \equiv \langle \sigma(r)\sigma(0) \rangle = n_i s / \pi (r^2 + 4s^2)^{3/2}. \quad (6)$$

The characteristic scales in the problem are as follows.⁶ The typical amplitude of fluctuations in σ is $\sqrt{n_i}/s$, see Eqs. (4) and (6). Their characteristic spatial scale is the spacer width s [cf. Eqs. (4-6) and Fig. 1]. In the cases studied below, $n_e \gtrsim n_p$ and $n_e \gg n_p$, s exceeds the average interelectron separation $a_0 = n_e^{-1/2}$. As usual in Coulomb problems, the energy is dominated by the longest scales, in this case s . The fluctuations $H_0(n) - H_0(n_e)$ of the the local energy density come from the interactions on the much shorter scale of $a_0 \ll s$ and can be treated as a perturbation.⁶ For the purpose of calculating the ground-state density profile $n(\mathbf{r})$ I neglect H_0 . Once such a ground state is known, I correct the total energy H by adding to it H_0 averaged over $n(\mathbf{r})$.

To find $n(\mathbf{r})$ one needs to solve the electrostatic problem with the following dual boundary conditions: if $n(\mathbf{r}) > 0$, then $\Phi(\mathbf{r}) = \mu = \text{const}$; otherwise, if $n = 0$ (DR), then^{6,7,14} $\Phi > \mu$. I start with the analysis of the large- n_e case, which clarifies why $\chi^{-1}(n_e)$ dependence is nonmonotonic and which provides a formula for the the density n_m where χ^{-1} has the minimum.

In the limit $n_e \gg \sqrt{n_i}/s$, the asymptotically exact treatment is possible because the DRs appear only in rare places where $\sigma(\mathbf{r})$ dips below $-n_e$. (In practice, this limit is realized when $n_e > K_0^{1/2} \approx 0.2\sqrt{n_i}/s$). The corresponding electrostatic problem is analogous to that of the metallic sheet perforated by small holes, see Fig. 1. The most elegant way to derive χ^{-1} in this regime is to calculate the fraction E_p/E_0 of the electric field that reaches the bottom layer in the geometry of Fig. 1. Indeed, E_p/E_0 is nonzero only if the probe layer is not a perfect metal, $\chi^{-1} \neq 0$. In the simplest case, where distances s_1 and s_2 are large, the following formula holds: $\chi^{-1} = 4\pi(e^2 s_2 / \kappa)(dE_p/dE_0)$ (cf. Ref. 9). This is essentially the formula used to deduce χ^{-1} in the experiment^{9,10,11,12}). It is immediately obvious that holes in the metallic sheet enhance the penetrated field E_p . For example, the field leaking through a round hole of radius

a is the field of a dipole¹⁵ $\mathbf{p} = (a^3/3\pi)\mathbf{E}_0$. If there is a finite but small concentration N_h of such holes, their fields are additive, leading to $\chi^{-1} = (8\pi e^2/3\kappa)N_h a^3$. From here the exact large- n_e asymptotics of χ^{-1} and μ can be obtained by substituting the proper N_h and averaging over the distribution of a . This can be done by noting that these holes appear around the minima of $\sigma(\mathbf{r})$ whose statistics is fixed by Eqs. (4-6). It is easy to see that the most probable holes are nearly perfect circles with radii⁶ $a \sim s\sqrt{K_0}/n_e$. The charge distribution around a single hole at distances $r > a$ is given by the formula

$$n(r) = \frac{\sigma_{xx} a^2}{\pi} \left[\sqrt{\frac{r^2}{a^2} - 1} - \left(\frac{r^2}{a^2} + \frac{2}{3} \right) \arccos \frac{a}{r} \right], \quad (7)$$

where the hole is assumed to be centered at $r = 0$ and $a^2 = -3[n_e + \sigma(0)]/\sigma_{xx}$. Equation (7) can be obtained, e.g., by generalizing the textbook solution¹⁵ for the hole in the metallic sheet¹⁶ and is also the limiting form of Eq. (11) in Ref. 17. Previously, Eq. (7) was used for study of quantum dots in Ref. 18.

In the current problem the main factor that determines the net contribution χ_{DR}^{-1} of the depletion holes to χ^{-1} is their exponentially small concentration, proportional to $P_1(-n_e) \propto \exp(-n_e^2/2K_0)$. The final result,

$$\chi_{\text{DR}}^{-1} \simeq (3\sqrt{2}/8\pi)(e^2 n_i / \kappa s n_e^2) \exp(-4\pi s^2 n_e^2 / n_i), \quad (8)$$

agrees with that of EPB but has no numerical coefficients left undetermined. To finalize the calculation, one needs to augment χ_{DR}^{-1} by the local term $\chi_0^{-1} = d^2\langle H_0(n) \rangle / dn_e^2$. In the present case, fluctuations around the average density are small. Hence, $\langle H_0(n) \rangle \simeq H_0(n_e)$ and

$$\chi_0^{-1}(n_e) \simeq -(e^2/\kappa)h_1(n_e)/\sqrt{n_e}, \quad n_e \gg \sqrt{n_i}/s, \quad (9)$$

where $h_1(n_e) = (3/4)h_0(n_e) + 3h_0' n_e + h_0'' n_e^2 \sim 1$.

Formula (8) implies a sharp upturn of the ITDOS as $n_e \rightarrow 0$ caused by the exponential growth of the DRs. At the boundary of its validity, $n_e \sim \sqrt{n_i}/s$, Eq. (8) gives $\chi_{\text{DR}}^{-1} \sim e^2 s / \kappa$, which is large and *positive*. On the other hand, the local term χ_0^{-1} [Eq. (9)] shows a weak dependence on n_e , remaining small and *negative*. Combined, they produce a strongly asymmetric minimum in $\chi^{-1}(n_e) = \chi_{\text{DR}}^{-1} + \chi_0^{-1}$ at the density

$$n_m = \frac{1}{4\sqrt{\pi}} \frac{\sqrt{n_i}}{s} \ln^{1/2} \left(\frac{4096}{\pi h_1^4} n_i s^2 \right). \quad (10)$$

The log-factor in Eq. (10) is rather insensitive to $n_i s^2$ and h_1 . For $n_i s^2 = h_1 = 1$, one gets $n_m \approx 0.38\sqrt{n_i}/s$. In comparison, (see Ref. 6 and below) the percolation threshold is

$$n_p \approx 0.12\sqrt{n_i}/s, \quad (11)$$

so that $n_m \approx 3n_p$. In accord with EPB's heuristic argument, at such density a very small area fraction is depleted (see inset in Fig. 2a), and so the use of the asymptotic formula (8) is justified.

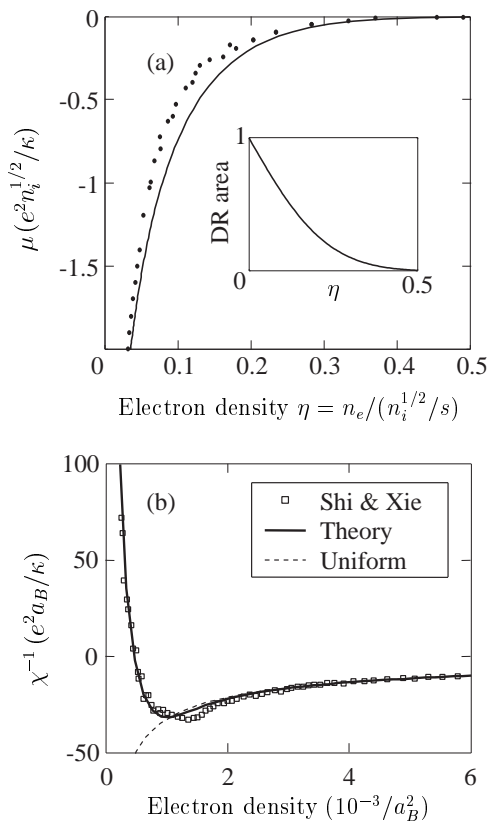


FIG. 2: (a) Electrochemical potential *vs.* electron density for the electrostatic problem, $H_0 \equiv 0$, according to the present theory (solid line) and EPB's numerical simulations (dots). Inset: Fraction of the depleted area *vs.* density. (b) χ^{-1} *vs.* density according to the numerical simulations of Shi and Xie⁸ (squares), the present theory (solid line), and for the uniform electron liquid (dashed line).

Let us now proceed to the case $n_e \sim n_p$. Again, I start with the electrostatic problem ($H_0 \equiv 0$). One expects DRs to be abundant and irregularly shaped. For a given n_e , the ground-state $n(\mathbf{r})$ is some nonlocal functional of σ and there is no hope to find it exactly. What I wish to report here is that a variational solution sought within the class of purely local functionals, $n(\mathbf{r}) = n[\sigma(\mathbf{r})]$ remarkably accurately reproduces the $\mu(n_e)$ and $\chi^{-1}(n_e)$ dependencies found in numerical work.^{6,8} More interestingly, it predicts the correct value of n_p [Eq. (11)].

The system of equation that defines such a variational state $n(\sigma)$ follows from the fact that for a Gaussian random function the averages over the total area L^2 of the system and over the distribution function are the same. This yields [cf. Eqs. (1–5)]

$$\frac{H_v}{L^2} = \frac{1}{2} \int \int d\sigma d\sigma' \rho(\sigma) G(\sigma, \sigma') \rho(\sigma'), \quad (12)$$

$$G(\sigma, \sigma') = \int d^2 r' V(r') [P_2(\sigma, \sigma') - P_1(\sigma) P_1(\sigma')], \quad (13)$$

where $\rho(\sigma) = n(\sigma) - n_e - \sigma$ and $V(r') = e^2/\kappa r'$. The

energy H_v needs to be minimized with respect to all functions $n(\sigma)$ that obey the constraints $n(\sigma) \geq 0$ and

$$\int d\sigma P_1(\sigma) n(\sigma) = n_e. \quad (14)$$

The latter ensures that the average density is equal to n_e . Introducing the Lagrange multiplier μ_v (variational estimate of the electrochemical potential), one obtains that H_v is minimized if, for all $\sigma > f$, $\rho(\sigma')$ satisfies

$$\int d\sigma' G(\sigma, \sigma') \rho(\sigma') = \mu_v(n_e) P_1(\sigma) \quad (15)$$

Here f is such that $n(f) = 0$. [I found that $n(\sigma)$ is always a monotonically increasing function, so that $n > 0$ corresponds to $\sigma > f$]. The kernel $G(\sigma, \sigma')$ [Eq. (13)] is log-divergent, $G \propto -\ln|\sigma - \sigma'|$ at $\sigma \rightarrow \sigma'$ and decays exponentially at large σ and σ' . There is a certain analogy between Eq. (15) and the integral equations of 1D electrostatics, which also have log-divergent kernels.^{15,18} This analogy entails that $n(\sigma) \sim \sqrt{\sigma - f}$ at σ close to f . Note that $\sigma(\mathbf{r}) - f$ is proportional to the distance in the real space between the given point \mathbf{r} and the boundary of the nearby DR. Thus, the variational principle renders correctly the square-root singularity in $n(\mathbf{r})$ at the edge of the DRs [cf., e.g., Eq (7)]. I was not able to establish the analytical form of the solution beyond this property and resorted to finding $n(\sigma)$ numerically. To do so the integral in Eq. (15) was converted into a discrete sum over 101 points on the interval $|\sigma| < 1.5\sqrt{n_i}/s$ the resultant system of 101 linear equations was solved on the computer. The solution can be approximated by a simple analytical *ansatz*

$$n_a(\sigma) = [(n_e + \sigma)^2 - (n_e + f)^2]^{1/2} \theta(\sigma - f), \quad (16)$$

where $\theta(z)$ is the step-function. For example, the energy H_v is nearly the same whether it is calculated using n_a or using the actual solution of Eq. (15). So, in principle, Eq. (16) obviates the need to solve Eq. (15). The only equation that needs to be solved is Eq. (14) for f .

At this point one can compare the predictions of the variational method for $\mu_v(n_e)$ with EPB's numerical results that were also obtained for the $H_0 = 0$ problem. As Fig. 2a illustrates, they are in a good agreement.¹⁹

To test the theory further I compare it next with the numerical data of Shi and Xie.⁸ To this end, one needs to calculate χ^{-1} including the effect of a finite H_0 . The first step is to take the derivative $\chi_{\text{DR}}^{-1} = d\mu_v/dn_e$, which is easily done numerically. An accurate fit to the result is provided by the interpolation formula

$$\chi_{\text{DR}}^{-1} \approx \frac{e^2 s 3\sqrt{2}}{\kappa} \frac{0.30 + \eta}{8\pi\eta 0.036 + 0.12\eta + \eta^2} \exp(-4\pi\eta^2), \quad (17)$$

where $\eta \equiv n_e s / \sqrt{n_i}$. This particular form is devised to match Eq. (8) at large n_e and is consistent up to log-corrections with the behavior expected^{7,20} at very small

n_e . The next step is to evaluate the quantity

$$\chi_0^{-1} = \frac{d^2}{dn_e^2} \langle H_0 \rangle = -\frac{d^2}{dn_e^2} \int_f^\infty d\sigma P_1(\sigma) H_0[n(\sigma)], \quad (18)$$

which is also easily done on the computer. The total ITDOS, $\chi^{-1}(n_e) = \chi_{\text{DR}}^{-1} + \chi_0^{-1}$, calculated from Eqs. (17–18) and the theoretical value of $n_m \sim 0.7 \times 10^{-3} a_B^{-2}$ [per Eq. (10)] compare very well with the simulations, see Fig. 2b. The parameters I used are $n_i = 6.25 \times 10^{-4} a_B^{-2}$ and $s = 10 a_B$, where a_B is the effective Bohr radius.²¹ In agreement with the exact results presented above, $\chi_0^{-1} \ll \chi_{\text{DR}}^{-1}$ at $n_e < n_m$, and so the upturn of χ^{-1} at low n_e is driven the growth of DRs.

Within the variational method the boundaries of the DRs coincide with the level lines $\sigma(\mathbf{r}) = f$ of the zero-mean random function σ . Consequently, the DRs percolate at $f \geq 0$. Solving Eq. (15) with $f = 0$, one arrives at Eq. (11), which is in excellent agreement with EPB's result $n_p \approx 0.11 \sqrt{n_i}/s$. One important quantity not reported in the published numerical works^{6,8} is the area fraction of the DR. Within the variational method, it is equal to $\text{erfc}(-f/\sqrt{2K_0})/2$, where $\text{erfc}(z)$ is the complementary error function. It is exactly 1/2 at $n_e = n_p$ and increases as $n_e \rightarrow 0$ as shown in Fig. 2a (inset).

Let us now compare our results with the experimental data. Taking a rough number $n_i = 3 \times 10^{11} \text{cm}^{-2}$ and a typical spacer width $s = 40 \text{nm}$ in Eq. (10), one gets $n_m \approx 5.2 \times 10^{10} \text{cm}^{-2}$, in agreement with observed values.¹⁰ The estimate for the percolation point is

$n_p \approx n_m/3 \approx 1.7 \times 10^{10} \text{cm}^{-2}$. Despite some small uncertainty in the last number (due to the uncertainties in n_i and h_1), n_p and n_m differ substantially, and so they can be easily distinguished experimentally. Therefore, the observed apparent MIT¹⁰ at $n = n_m$ has nothing to do with the percolation of the DRs and moreover with breaking of the electron liquid into droplets (the latter occurs at $n_e \ll n_p$). From Fig. 2a, one can estimate that the DR occupy mere 6% of the total area at $n = n_m$.

One qualitative prediction that follows from Eqs. (9) and (17) is that the upturn of $\chi^{-1}(n_e)$ should be sharper in samples with larger s , which seems to be the case if the data of Ref. 9 ($s = 14 \text{nm}$) are compared with those of Refs. 10,11,12 ($s \leq 4 \text{nm}$). Detailed fits are left for future.

I conclude with mentioning some other theoretical work on the subject. It was suggested²² that near the MIT, function $\chi^{-1}(n_e)$ may contain both regular and singular parts. My theory can be considered the calculation of the former. Its detailed comparison with experiment may furnish an estimate of the putative singular term. The effect of disorder on χ^{-1} was also studied in Refs. 23 and 24 but the electron density inhomogeneity was not accounted for. Finally, a nonmonotonic $\chi^{-1}(n_e)$ dependence was found in a model²⁵ without disorder.

This work is supported by C. & W. Hellman Fund and A. P. Sloan Foundation. I am grateful to B. I. Shklovskii for indispensable comments and insights, and also to H. W. Jiang, A. K. Savchenko, and J. Shi for discussions.

¹ For review, see E. Abrahams, S. V. Kravchenko, and M. P. Sarachik, *Rev. Mod. Phys.* **73**, 251 (2001).
² G. Eytan, Y. Yayon, M. Rappaport, H. Shtrikman, and I. Bar-Joseph, *Phys. Rev. Lett.* **81**, 1666 (1998).
³ G. Finkelstein, P. I. Glicofridis, R. C. Ashoori, and M. Shayegan, *Science* **289**, 90 (2000).
⁴ S. Ilani, A. Yacoby, D. Mahalu, and H. Shtrikman, *Phys. Rev. Lett.* **84**, 3133 (2000); *Science* **292**, 1354 (2001).
⁵ M. Morgenstern, Chr. Wittneven, R. Dombrowski, and R. Wiesendanger, *Phys. Rev. Lett.* **84**, 5588 (2000).
⁶ A. L. Efros, F. G. Pikus, and V. G. Burnett, *Phys. Rev. B* **47**, 2233 (1993) and references therein.
⁷ A. L. Efros and B. I. Shklovskii, *Electronic Properties of Doped Semiconductors* (Springer, New York, 1984); B. I. Shklovskii and A. L. Efros, *JETP Lett.* **44**, 669 (1986).
⁸ J. Shi and X. C. Xie, *Phys. Rev. Lett.* **88**, 86401 (2002).
⁹ J. P. Eisenstein, L. N. Pfeiffer, and K. W. West, *Phys. Rev. B* **50**, 1760 (1994).
¹⁰ S. C. Dultz and H. W. Jiang, *Phys. Rev. Lett.* **84**, 4689 (2000).
¹¹ S. C. Dultz, B. Alavi, and H. W. Jiang, *cond-mat/0210584*.
¹² G. D. Allison, A. K. Savchenko, and E. H. Linfield, *Proceedings the 26th Intl. Conf. on Physics of Semiconductors* (Edinburgh, 2002).
¹³ B. Tanatar and D. M. Ceperley, *Phys. Rev. B* **39**, 5005 (1989).

¹⁴ M. M. Fogler, *cond-mat/0402458*.

¹⁵ L. D. Landau and E. M. Lifshitz, *Electrodynamics of Continuous Media* (Pergamon, New York, 1960).

¹⁶ Note that $E_0 = 4\pi\sigma(0)/\kappa + \text{const}$ and that p can be read off the asymptotic law $2\pi\sigma(r) \sim -p/r^3$ valid at $r \gg a$. This leads to the same formula for χ^{-1} as in the case of a hole in a metallic sheet, see more details in Ref. 14.

¹⁷ V. G. Burnett, A. L. Efros, and F. G. Pikus, *Phys. Rev. B* **48**, 14365 (1993).

¹⁸ M. M. Fogler, E. I. Levin, and B. I. Shklovskii, *Phys. Rev. B* **49**, 13767 (1994).

¹⁹ This is also true in several other geometries, see Ref. 14.

²⁰ V. A. Gergel' and R. A. Suris, *Sov. Phys. JETP* **48**, 95 (1978).

²¹ The data in Ref. 8 must be divided by two to correct a notational error (J. Shi, private communication); n_i is four times smaller than in Ref. 8 to account for a peculiar choice $q = e/2$ of the impurity charge made there.

²² S. Chakravarty, S. Kivelson, C. Nayak, and K. Voelker, *Phil. Mag. B* **79**, 859 (1999).

²³ Q. Si and C. M. Varma, *Phys. Rev. Lett.* **81**, 4951 (1998).

²⁴ R. Asgari and B. Tanatar, *Phys. Rev. B* **65**, 085311 (2002).

²⁵ S. Orozco, R. M. Méndez-Moreno, and M. Moreno, *Phys. Rev. B* **67**, 195109 (2003).